# HOKKAIDO UNIVERSITY

| | |
|---|---|
| Title | PLC-based LP11 mode rotator for mode-division multiplexing transmission |
| Author(s) | Saitoh, Kunimasa; Uematsu, Takui; Hanzawa, Nobutomo; Ishizaka, Yuhei; Masumoto, Kohei; Sakamoto, Taiji; Matsui, Takashi; Tsujikawa, Kyozo; Yamamoto, Fumihiko |
| Citation | Optics Express, 22(16), 19117-19130<br>https://doi.org/10.1364/OE.22.019117 |
| Issue Date | 2014-08-11 |
| Doc URL | http://hdl.handle.net/2115/57418 |
| Rights | ©2014 Optical Society of America. One print or electronic copy may be made for personal use only. Systematic reproduction and distribution, duplication of any material in this paper for a fee or for commercial purposes, or modifications of the content of this paper are prohibited. |
| Type | article |
| File Information | oe-22-16-19117.pdf |

# PLC-based LP$_{11}$ mode rotator for mode-division multiplexing transmission

**Kunimasa Saitoh,[1,*] Takui Uematsu,[1] Nobutomo Hanzawa,[2] Yuhei Ishizaka,[1] Kohei Masumoto,[1] Taiji Sakamoto,[2] Takashi Matsui,[2] Kyozo Tsujikawa,[2] and Fumihiko Yamamoto[2]**

[1]*Graduate School of Information Science and Technology, Hokkaido University, Sapporo 060-0814, Japan*
[2]*NTT Access Network Service Systems Laboratories, NTT Corporation, 1-7-1 Hanabatake, Ibaraki 305-0805, Japan*
[*]*ksaitoh@ist.hokudai.ac.jp*

**Abstract:** A PLC-based LP$_{11}$ mode rotator is proposed. The proposed mode rotator is composed of a waveguide with a trench that provides asymmetry of the waveguide. Numerical simulations show that converting LP$_{11a}$ (LP$_{11b}$) mode to LP$_{11b}$ (LP$_{11a}$) mode can be achieved with high conversion efficiency (more than 90%) and little polarization dependence over a wide wavelength range from 1450 nm to 1650 nm. In addition, we fabricate the proposed LP$_{11}$ mode rotator using silica-based PLC. It is confirmed that the fabricated mode rotator can convert LP$_{11a}$ mode to LP$_{11b}$ mode over a wide wavelength range.

## References and links

1. E. Ip, N. Bai, Y.-K. Huang, E. Mateo, F. Yaman, M.-J. Li, S. Bickham, S. Ten, J. Liñares, C. Montero, V. Moreno, X. Prieto, Y. Luo, G. D. Peng, G. Li, and T. Wang, "6 × 6 MIMO transmission over 50+25+10 km heterogeneous spans of few-mode fiber with inline erbium-doped fiber amplifier," in *Optical Fiber Communication Conference/National Fiber Engineers Conference* 2012, OSA Technical Digest (online) (Optical Society of America, 2012), paper OTu2C.4. *http://ieeexplore.ieee.org/xpls/abs_all.jsp?arnumber=6192056*
2. R. Ryf, S. Randel, A. H. Gnauck, C. Bolle, A. Sierra, S. Mumtaz, M. Esmaeelpour, E. C. Burrows, R.-J. Essiambre, P. J. Winzer, D. W. Peckham, A. H. McCurdy, and R. Lingle, "Mode-division multiplexing over 96 km of few-mode fiber using coherent 6 × 6 MIMO processing," J. Lightwave Technol. **30**(4), 521–531 (2012).
3. M. Salsi, C. Koebele, D. Sperti, P. Tran, H. Mardoyan, P. Brindel, S. Bigo, A. Boutin, F. Verluise, P. Sillard, M. B. Astruc, L. Provost, and G. Charlet, "Mode-division multiplexing of 2 × 100 Gb/s channels using an LCOS-based spatial modulator," J. Lightwave Technol. **30**(4), 618–623 (2012).
4. N. Hanzawa, K. Saitoh, T. Sakamoto, T. Matsui, S. Tomita, and M. Koshiba, "Mode-division multiplexed transmission with fiber mode couplers," in *Optical Fiber Communication Conference/National Fiber Engineers Conference* 2012, OSA Technical Digest (online) (Optical Society of America, 2012), paper OW1D.4.
5. A. Li, J. Ye, X. Chen, and W. Shieh, "Low-loss fused mode coupler for few-mode transmission," in *Optical Fiber Communication Conference/National Fiber Engineers Conference* 2013, OSA Technical Digest (online) (Optical Society of America, 2013), paper OTu3G.4.
6. S. G. Leon-Saval, N. K. Fontaine, J. R. Salazar-Gil, B. Ercan, R. Ryf, and J. Bland-Hawthorn, "Mode-selective photonic lanterns for space-division multiplexing," Opt. Express **22**(1), 1036–1044 (2014).
7. S. Yerolatsitis, I. Gris-Sánchez, and T. A. Birks, "Adiabatically-tapered fiber mode multiplexers," Opt. Express **22**(1), 608–617 (2014).
8. N. Hanzawa, K. Saitoh, T. Sakamoto, T. Matsui, K. Tsujikawa, M. Koshiba, and F. Yamamoto, "Two-mode PLC-based mode multi/demultiplexer for mode and wavelength division multiplexed transmission," Opt. Express **21**(22), 25752–25760 (2013).
9. T. Uematsu, K. Saitoh, N. Hanzawa, T. Sakamoto, T. Matsui, K. Tsujikawa, and M. Koshiba, "Low-loss and broadband PLC-type mode (de)multiplexer for mode-division multiplexing transmission," in *Optical Fiber Communication Conference/National Fiber Engineers Conference* 2013, OSA Technical Digest (online) (Optical Society of America, 2013), paper OTh1B.5.
10. N. Hanzawa, K. Saitoh, T. Sakamoto, K. Tsujikawa, T. Uematsu, M. Koshiba, and F. Yamamoto, "Three-mode PLC-type multi/demultiplexer for mode-division multiplexing transmission," in *European Conference and Exhibition on Optical Communication* 2013, OSA Technical Digest (online) (Optical Society of America, 2013), paper Tu.1.B.3. *http://ieeexplore.ieee.org/xpls/abs_all.jsp?arnumber=6647527*
11. T. Uematsu, N. Hanzawa, K. Saitoh, Y. Ishizaka, K. Masumoto, T. Sakamoto, T. Matsui, K. Tsujikawa, and F. Yamamoto, "PLC-type LP$_{11}$ mode rotator with single-trench waveguide for mode-division multiplexing

transmission," in *Optical Fiber Communication Conference/National Fiber Engineers Conference* 2014, OSA Technical Digest (online) (Optical Society of America, 2014), paper Th2A.52.

12. K. Saitoh and M. Koshiba, "Full-vectorial finite element beam propagation method with perfectly matched layers for anisotropic optical waveguides," J. Lightwave Technol. **19**(3), 405–413 (2001).

## 1. Introduction

An expansion of the transmission capacity per fiber is needed because of the rapid growth of Internet traffic in the optical fiber network. Mode-division multiplexing (MDM) has attracted attention to obtain a much larger transmission capacity. The mode (de)multiplexer is an important component to realize MDM transmission. Various mode (de)multiplexers based on free-space optics [1–3], fiber coupler and a long-period fiber bragg grating (LPFBG) [4,5], photonic lantern [6], adiabatically-tapered fiber [7], and planar lightwave circuit (PLC) [8,9] have been demonstrated.

PLC-based mode (de)multiplexer has unique advantages including a low insertion loss, relatively low wavelength dependence, a small size, and high mass productivity due to the adoption of mature semiconductor manufacturing technologies such as photolithography and ion etching. The PLC-based mode (de)multiplexer is one of the promising mode (de)multiplexers for the purpose of mass production. We have proposed the PLC-based three-mode multiplexer which can multiplex and excite $LP_{01}$, $LP_{11a}$, and $LP_{21}$ modes [10]. The PLC-based mode multiplexer which can excite $LP_{11b}$ mode is required to realize a mode (de)multiplexer which can multiplex $LP_{01}$, $LP_{11a}$, $LP_{11b}$, and $LP_{21}$ modes. However, the PLC-type mode multiplexer which can excite $LP_{11b}$ mode has not been presented because it is difficult to excite electronic waveguide modes $E_{mn}$ ($n \geq 2$) like $LP_{11b}$ mode in the same plane.

In this paper, we design and fabricate a PLC-based $LP_{11}$ mode rotator for the excitation of $LP_{11b}$ mode [11]. Numerical simulations show that converting $LP_{11a}$ mode to $LP_{11b}$ mode can be achieved with high conversion efficiency (more than 90%) over a wide wavelength range from 1450 nm to 1650 nm. Numerical simulations also show that the $LP_{11}$ mode rotator can convert $LP_{11b}$ mode to $LP_{11a}$ mode, has little polarization dependence, and has a good fabrication tolerance. We finally fabricate the proposed $LP_{11}$ mode rotator using silica-based PLC and confirm that the fabricated $LP_{11}$ mode rotator can convert $LP_{11a}$ mode to $LP_{11b}$ mode over a wide wavelength range.

## 2. Principle and design

Figure 1 shows the structure of the PLC-based $LP_{11}$ mode rotator. The proposed mode rotator is composed of a waveguide with a trench that provides asymmetry of the waveguide as shown in Fig. 1. The degree of the asymmetry can be controlled by changing the trench position $t$, the trench width $s$, and the trench depth $d$. By properly designing the trench parameters, two orthogonal $LP_{11}$ modes whose optical axes are rotated by around 45° with respect to the $x$- and $y$-axes propagate in the waveguide with the trench as shown in Figs. 2(a) and 2(b), and the two orthogonal $LP_{11}$ modes are equally excited and propagated with different propagation constants, $\beta_1$ and $\beta_2$, in the waveguide with the trench when $LP_{11a}$ ($LP_{11b}$) mode is launched. By setting the length of the waveguide with the trench to a half beat-length, $\pi/(\beta_1 - \beta_2)$, $LP_{11a}$ ($LP_{11b}$) mode is rotated into $LP_{11b}$ ($LP_{11a}$) mode.
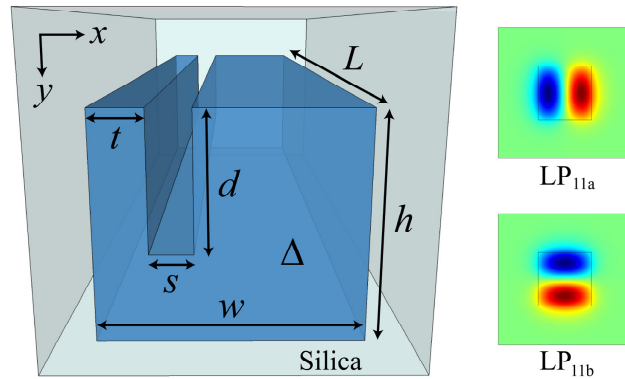
Fig. 1. Structure of a PLC-based $LP_{11}$ mode rotator with a trench. Inset images show field distributions of $LP_{11a}$ and $LP_{11b}$ modes.
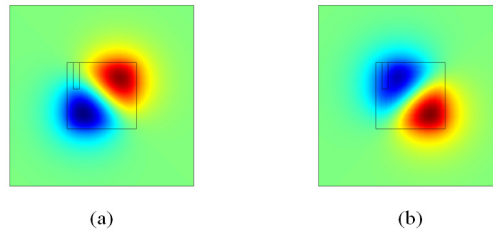


(a)              (b)

Fig. 2. Field distributions of two orthogonal $LP_{11}$ modes whose optical axes are rotated with respect to the $x$- and $y$-axes in the waveguide with the trench; (a) 1st $LP_{11}$ mode, (b) 2nd $LP_{11}$ mode.

In this paper, we assume that the proposed mode rotator is based on silica-based PLC with a relative refractive index difference $\Delta$ between the core and cladding of 0.45% [10], and the waveguide width $w$ and height $h$ are respectively set to $w = 11.3$ μm and $h = 11.0$ μm in order to reduce the coupling loss between PLC waveguide and a two-mode fiber to be connected. One can choose other values for $\Delta$, $w$, and $h$ as you desire.

Next, we choose design parameters related to the trench such as the trench position $t$, width $s$, and depth $d$. When $t$, $d$, and $s$ are chosen to large values, the device length tends to be short because the difference of the propagation constants, $\beta_1$ and $\beta_2$, between two orthogonal $LP_{11}$ modes becomes larger. However, crosstalk to undesired modes such as $LP_{01}$ mode and undesired back reflections become higher when $t$, $d$, and $s$ are chosen to large values due to the mode field mismatch at the boundary between the waveguides with and without the trench. Thus, $t$, $d$, and $s$ should be chosen to small values in order to suppress the crosstalk to undesired modes. In this paper, we chose target parameters of $t = 2.0$ μm and $s = 1.5$ μm for easy fabrication. Figure 3(a) shows $d$ dependence of the normalized overlap integral of $LP_{11a}$ mode with 1st and 2nd $LP_{11}$ modes shown in Fig. 2 at a wavelength of 1550 nm, where $t = 2.0$ μm and $s = 1.5$ μm. From Fig. 3(a), $d$ should be chosen to $d = 5.4$ μm for the overlap of $LP_{11a}$ mode with the two orthogonal $LP_{11}$ modes shown in Fig. 2 to be equivalent. Figure 3(b) shows $t$ dependence of the normalized overlap integral of $LP_{11a}$ mode with 1st and 2nd $LP_{11}$ modes at a wavelength of 1550 nm with $d = 5.4$ μm and $s = 1.5$ μm, and Fig. 3(c) shows $s$ dependence of the normalized overlap integral of $LP_{11a}$ mode with 1st and 2nd $LP_{11}$ modes at a wavelength of 1550 nm with $d = 5.4$ μm and $t = 2.0$ μm. It can be seen that the normalized overlap integral of $LP_{11a}$ mode with 1st and 2nd $LP_{11}$ modes can be controlled by changing $t$, $d$, and $s$. Finally, the length of the mode rotator $L$ is set to $L = 1.46$ mm, which equals the half beat-length of the two orthogonal $LP_{11}$ modes shown in Fig. 2. The designed parameters are

shown in Table 1. It has been numerically confirmed that the undesired back reflection at the boundary between the waveguides with and without the trench is lower than −30 dB when the designed parameters in Table 1 are used.
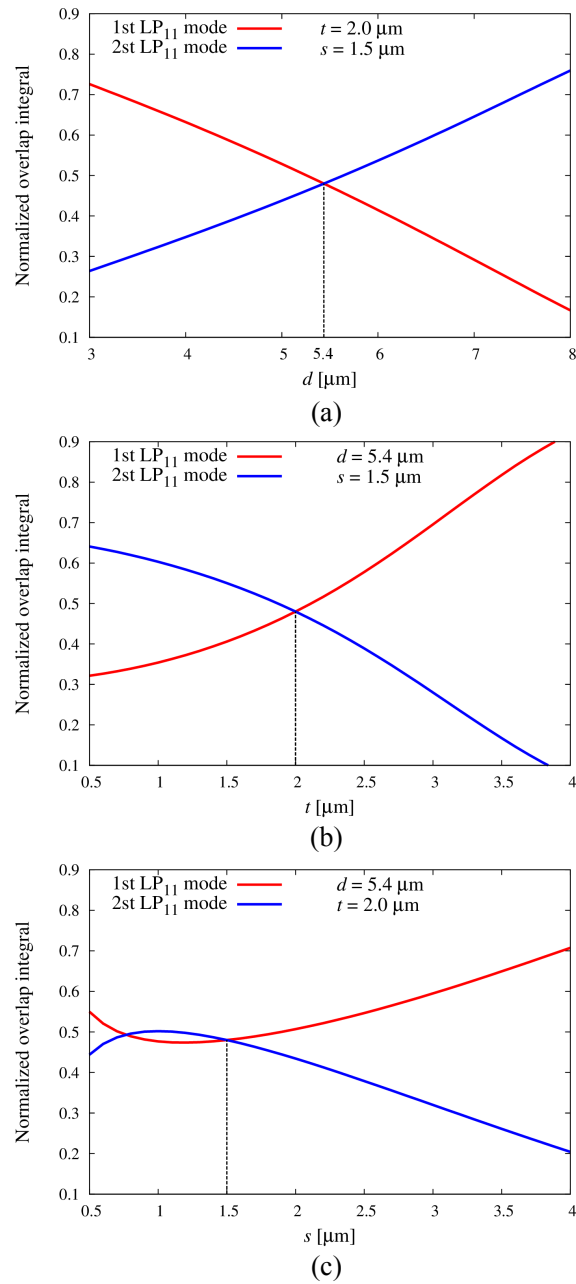


(a)



(b)



(c)

Fig. 3. (a) Trench depth $d$, (b) trench position $t$, and (c) trench width $s$ dependence of normalized overlap integral of 1st and 2nd $LP_{11}$ modes shown in Fig. 2 with $LP_{11a}$ mode at a wavelength of 1550 nm.

Figure 4 shows the calculated conversion efficiency as a function of the length of the proposed mode rotator for $x$- and $y$- polarization when (a) $LP_{11a}$ mode or (b) $LP_{11b}$ mode is input at a wavelength of 1550 nm. The inset images show the field distributions of $LP_{11}$ mode

in the mode rotator at each propagation length. Red and blue solid lines show the result for *x*-polarization. Green and cyan dashed lines show the result for *y*-polarization. We used the full-vector finite-element beam propagation method [12] for numerical simulations. From Fig. 4, we can see that $LP_{11a}$ ($LP_{11b}$) mode is converted into $LP_{11b}$ ($LP_{11a}$) when *L* equals 1.46 mm, and there is little polarization dependence because two lines for *x*- and *y*- polarization almost overlap each other. The polarization dependence in the PLC-based mode rotator with small index difference between core and cladding is negligibly small, however, it may become large if the core-cladding index difference increases.

**Table 1. Design Parameters of the Proposed $LP_{11}$ Mode Rotator.**

| Δ | *w* | *h* | *L* | *t* | *d* | *s* |
|---|-----|-----|-----|-----|-----|-----|
| 0.45% | 11.3 μm | 11.0 μm | 1460 μm | 2.0 μm | 5.4 μm | 1.5 μm |



(a)



(b)
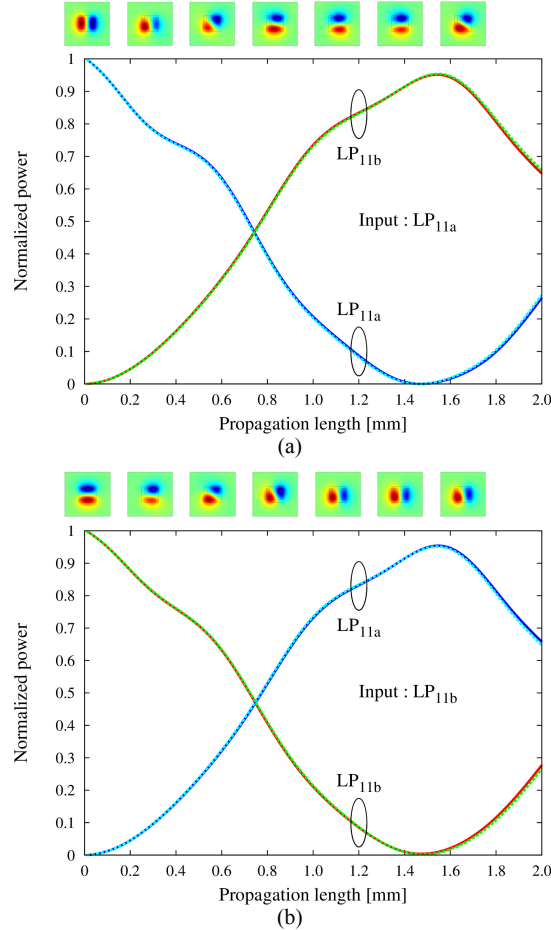
Fig. 4. Conversion efficiency as a function of the trench waveguide length for *x*- and *y*-polarization when (a) $LP_{11a}$ mode or (b) $LP_{11b}$ mode is input at a wavelength of 1550 nm. Inset images show field distributions of $LP_{11}$ mode in the $LP_{11}$ mode rotator. Red and blue solid lines show the results for *x*-polarization. Green and cyan dashed lines show the results for *y*-polarization. Two lines almost overlap each other owing to little polarization dependence. See Media 1.
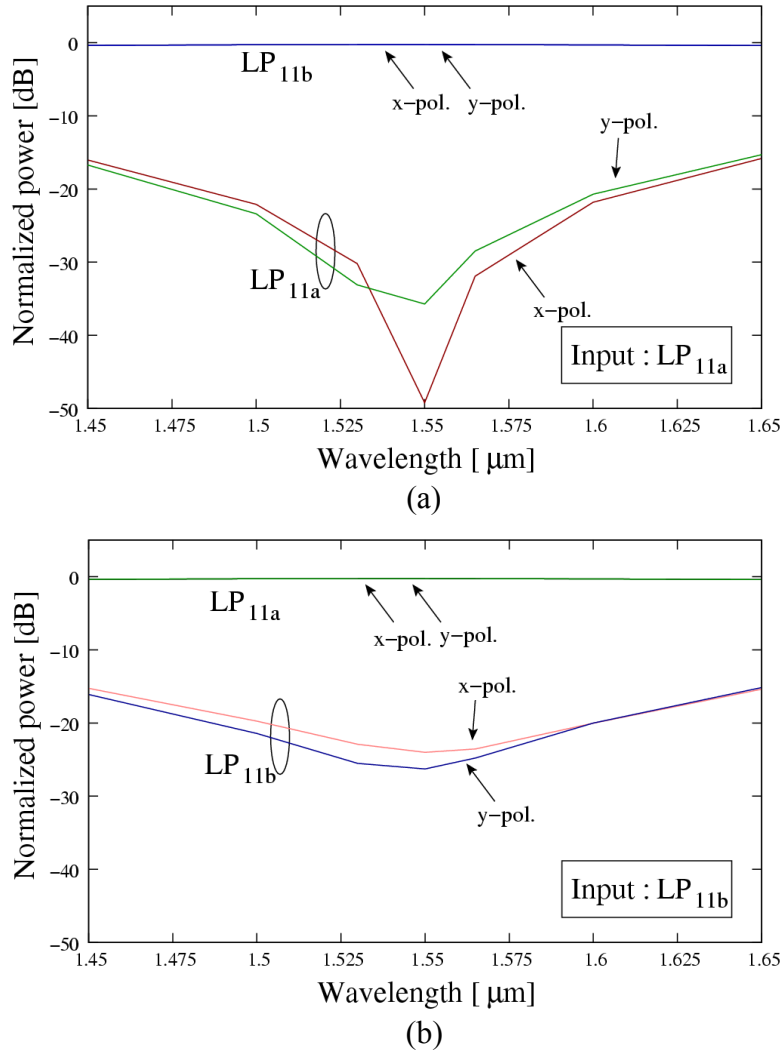
Fig. 5. Wavelength dependence of the $LP_{11}$ mode rotator when (a) $LP_{11a}$ mode or (b) $LP_{11b}$ mode is input.

## 3. Characteristics

Figure 5 shows the calculated wavelength dependence of the $LP_{11}$ mode rotator when (a) $LP_{11a}$ mode or (b) $LP_{11b}$ mode is launched into the mode rotator with the design parameters shown in Table 1. From Fig. 5, the wavelength dependence of the conversion efficiency is negligible (more than 90% over a wavelength range from 1.45 μm to 1.65 μm), and the crosstalk to the input $LP_{11}$ mode is less than −20 dB over a wavelength range from 1.5 μm to 1.6 μm for both polarizations.

Figure 6 shows the fabrication tolerance of the $LP_{11}$ mode rotator when $LP_{11a}$ mode is launched at a wavelength of 1550 nm. The conversion efficiency is insensitive to fabrication errors and the crosstalk to the input $LP_{11}$ mode is less than −20 dB when $t$, $d$, and $s$ change by ± 0.3 μm, ± 0.4 μm, and ± 0.1 μm, respectively. The actual fluctuation through PLC fabrication will depend on a fabrication process and it is usually in the order of submicron.
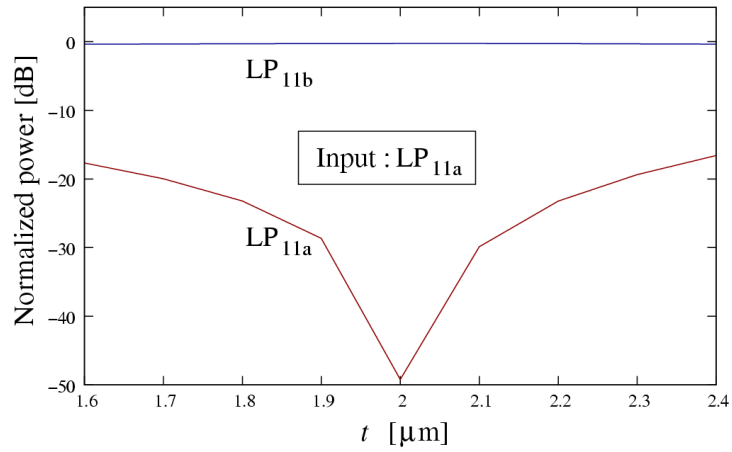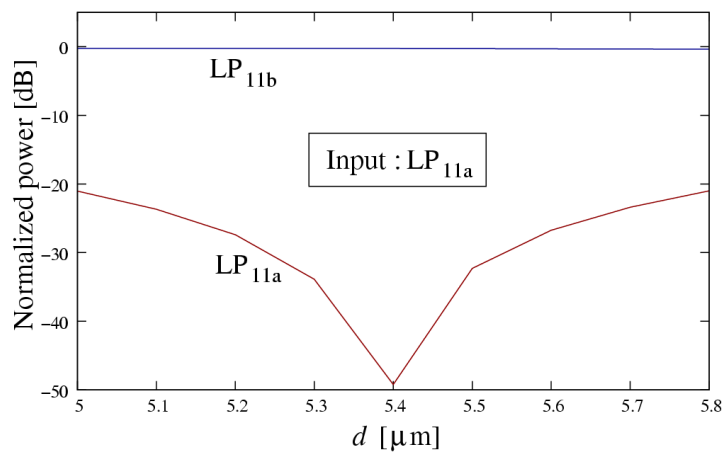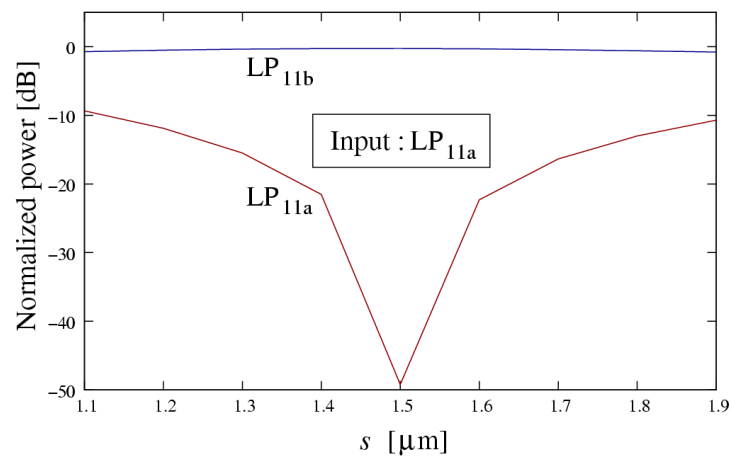
Fig. 6. Fabrication tolerance to (a) trench position $t$, (b) trench depth $d$, (c) trench width $s$ when LP$_{11a}$ mode is input at a wavelength of 1550 nm.
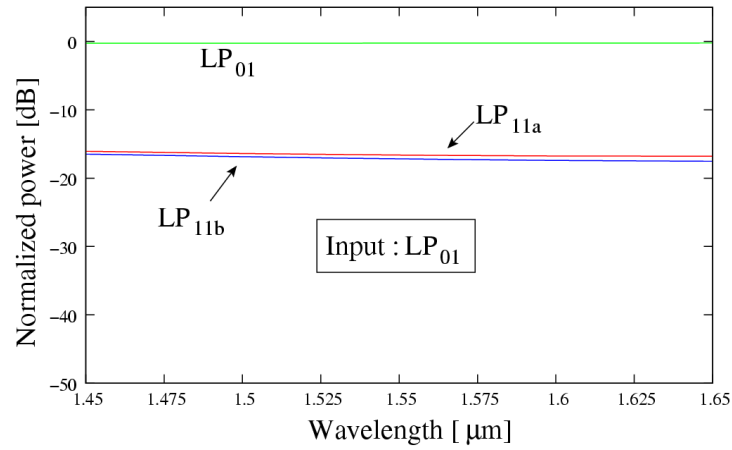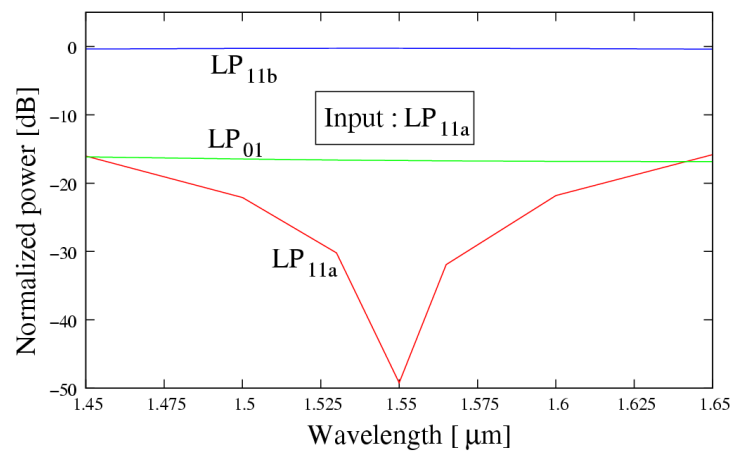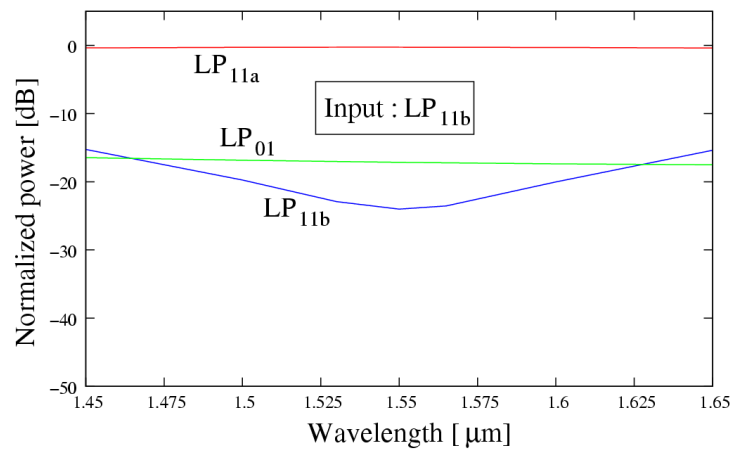
Fig. 7. Wavelength dependence of the normalized output power of $LP_{01}$, $LP_{11a}$, and $LP_{11b}$ modes for the case of the design parameters shown in Table 1 ($t = 2.0$ μm, $d = 5.4$ μm, and $L = 1.46$ mm) when (a) $LP_{01}$ mode, (b) $LP_{11a}$ mode, or (c) $LP_{11b}$ mode is launched.
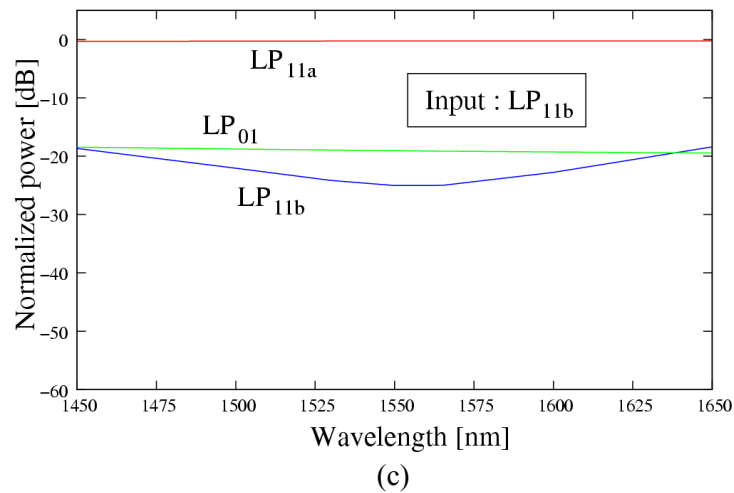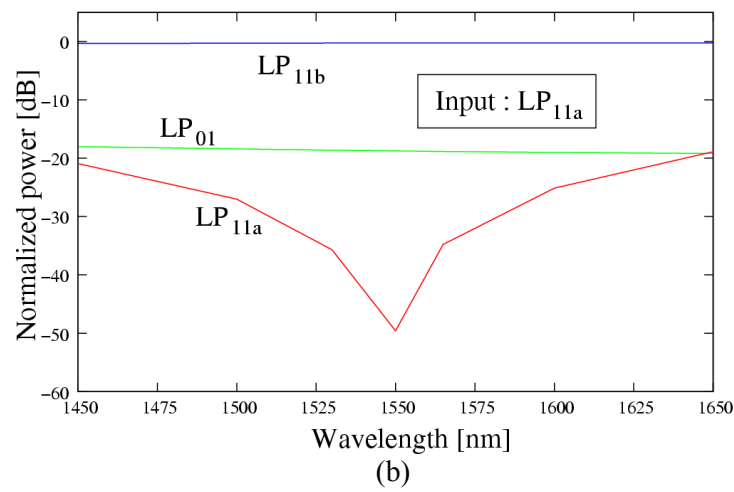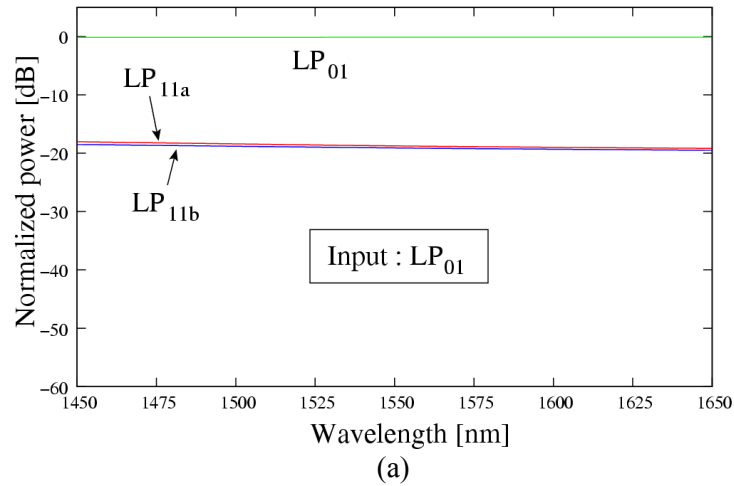
Fig. 8. Wavelength dependence of the normalized output power for the case of $t$ = 1.0 μm, $d$ = 4.3 μm, and $L$ = 1.92 mm (the other parameters are not changed) when (a) $LP_{01}$ mode, (b) $LP_{11a}$ mode, or (c) $LP_{11b}$ mode is launched.
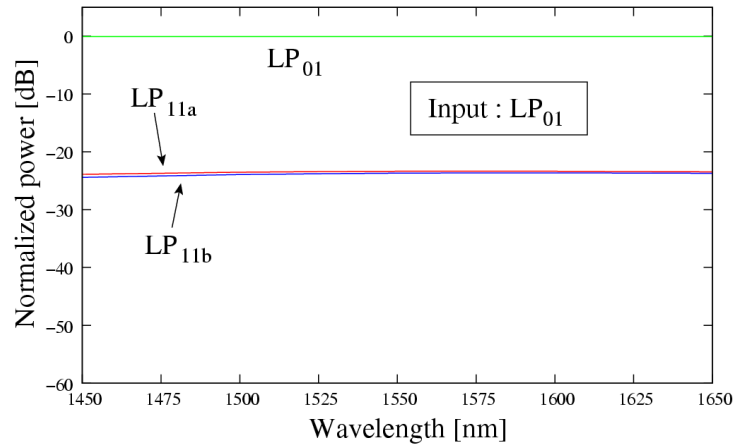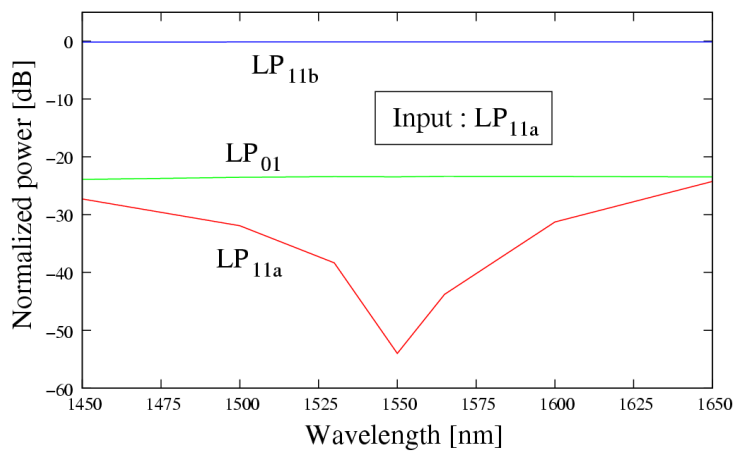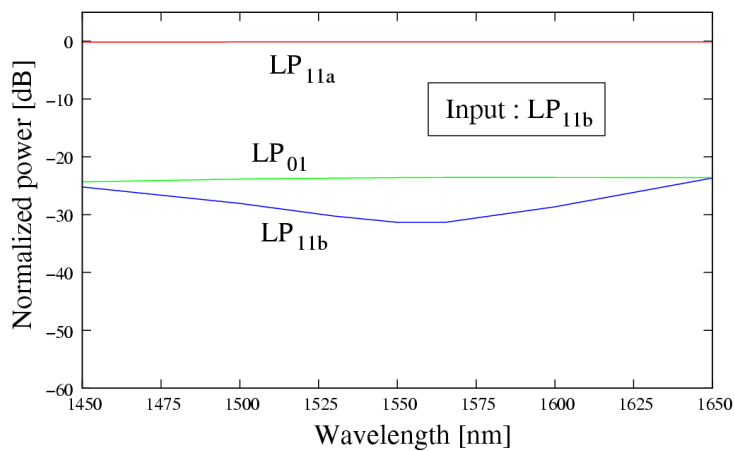
Fig. 9. Wavelength dependence of the normalized output power for the case of $t = 0$ μm, $d = 3.9$ μm, and $L = 2.99$ mm (the other parameters are not changed) when (a) $LP_{01}$ mode, (b) $LP_{11a}$ mode, or (c) $LP_{11b}$ mode is launched.

Next, we consider reducing the crosstalk to undesired modes such as $LP_{01}$ mode and the input $LP_{11}$ mode. Figure 7 shows the calculated wavelength dependence of the normalized output power of $LP_{01}$, $LP_{11a}$, and $LP_{11b}$ modes when (a) $LP_{01}$ mode, (b) $LP_{11a}$ mode, or (c) $LP_{11b}$ mode is launched into the mode rotator with the design parameters shown in Table 1. From Fig. 7(a), $LP_{01}$ mode is output (without polarization conversion) when $LP_{01}$ mode is input. This is because the optical axis for the $LP_{01}$ mode is not rotated by the small trench. As shown in Fig. 7, the crosstalk to the undesired modes is less than −16 dB over a wavelength range from 1.45 μm to 1.65 μm.

The crosstalk can be improved by making the parameters related to the trench smaller values. Figure 8 shows the calculated wavelength dependence of the normalized output power of $LP_{01}$, $LP_{11a}$, and $LP_{11b}$ modes for the case of $t = 1.0$ μm, $d = 4.3$ μm, and $L = 1.92$ mm (the other parameters are not changed) when (a) $LP_{01}$ mode, (b) $LP_{11a}$ mode, or (c) $LP_{11b}$ mode is launched. From Figs. 7 and 8, we can see that the crosstalk to the undesired modes is reduced from −16 dB to −18 dB when the trench parameters are set to be smaller values.

Figure 9 shows the calculated wavelength dependence of the normalized output power of $LP_{01}$, $LP_{11a}$, and $LP_{11b}$ modes for the case of $t = 0$ μm, $d = 3.9$ μm, and $L = 2.99$ mm (the other parameters are not changed) when (a) $LP_{01}$ mode, (b) $LP_{11a}$ mode, or (c) $LP_{11b}$ mode is launched. The crosstalk to the undesired modes is reduced from −16 dB to −23 dB when the trench parameters are set to be smaller values as shown in Figs. 7 and 9.
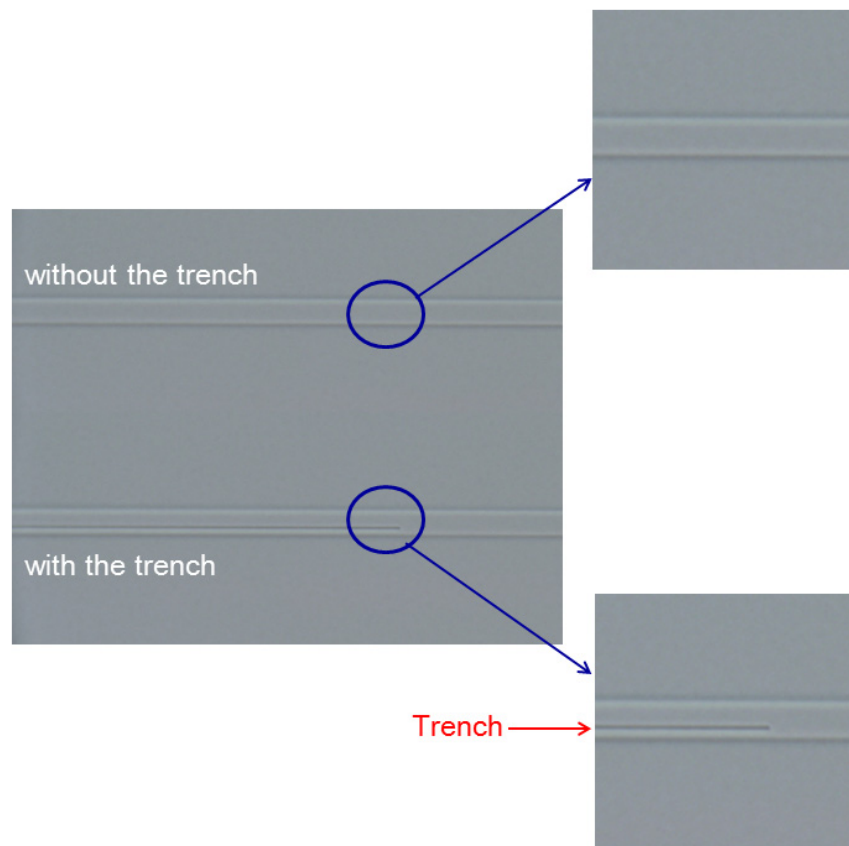


Fig. 10. Fabricated $LP_{11}$ mode rotator with silica-based PLC. All components are fabricated on a chip. Upper and lower waveguides do not have and have the trench, respectively.
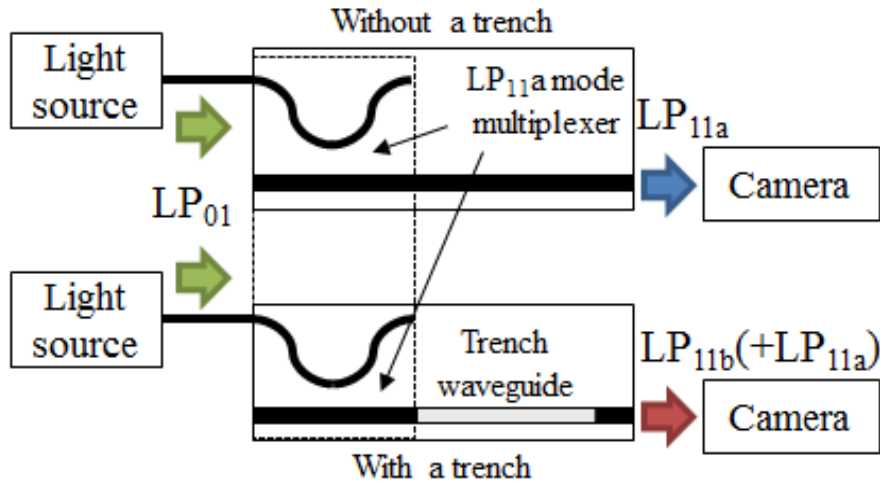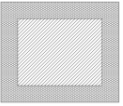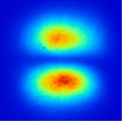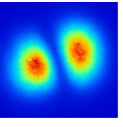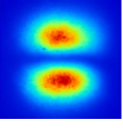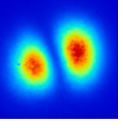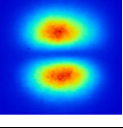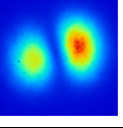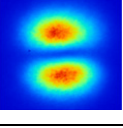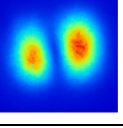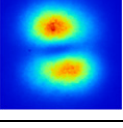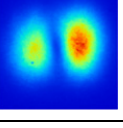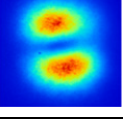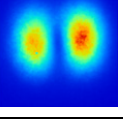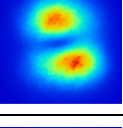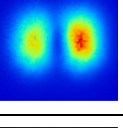
Fig. 11. Experimental setup for the $LP_{11}$ mode rotator. PLC-based mode multiplexers are used for excitation of $LP_{11a}$ mode.

## 4. Fabrication

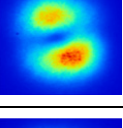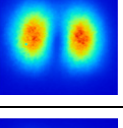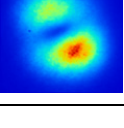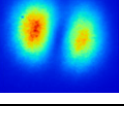Figure 10 shows the fabricated $LP_{11}$ mode rotator using silica-based PLC with the target structural parameters shown in Table 1. All components shown in Fig. 10 are fabricated on a chip. Figure 11 shows the experimental setup for the $LP_{11}$ mode rotator. In the experiment, we observed near field patterns of output light through a waveguide with or without the trench when $LP_{11a}$ mode is input. $LP_{11a}$ mode should be output when $LP_{11a}$ mode is input to the waveguide without the trench. On the other hand, rotated $LP_{11}$ mode (ideally $LP_{11b}$ mode) should be output when $LP_{11a}$ mode is input to the waveguide with the trench. We used the PLC-based two-mode multiplexer [8] to excite $LP_{11a}$ mode. Table 2 shows the near field patterns of output light through the waveguide with (the left column of Table 2) or without (the right column of Table 2) the trench when $LP_{11a}$ mode is input at each wavelength. The reason of rotation of $LP_{11}$ mode with the change of wavelength is because the optimum half beat-length for 90 degree rotation is depending on the wavelength. From Table 2, we can confirm that the fabricated $LP_{11}$ mode rotator converts $LP_{11a}$ mode to $LP_{11b}$ mode over a wide wavelength range from 1460 nm to 1600 nm.

We can obtain PLC-based three-mode (de)multiplexer for $LP_{01}$, $LP_{11a}$, and $LP_{11b}$ modes when we utilize the proposed $LP_{11}$ mode rotator and the two-mode (de)multiplexer [8]. Figure 12 illustrates the schematic drawing of the PLC-based three-mode multiplexer that can multiplex and demultiplex $LP_{01}$, $LP_{11a}$, and $LP_{11b}$ modes. The three-mode multiplexer consists of two PLC-based two-mode multiplexers [8] and the proposed $LP_{11}$ mode rotator. Two-mode multiplexers are used for excitation of $LP_{11a}$ mode. All components can be fabricated on a chip. $LP_{11b}$, $LP_{01}$, and $LP_{11a}$ modes are output when $LP_{01}$ modes are launched to port 1, port 2, and port3, respectively.

**Table 2. Near Field Patterns of Output Light Through the Fabricated Waveguide with (Left) or without (Right) a Trench when LP$_{11a}$ Mode is Input at Each Wavelength**

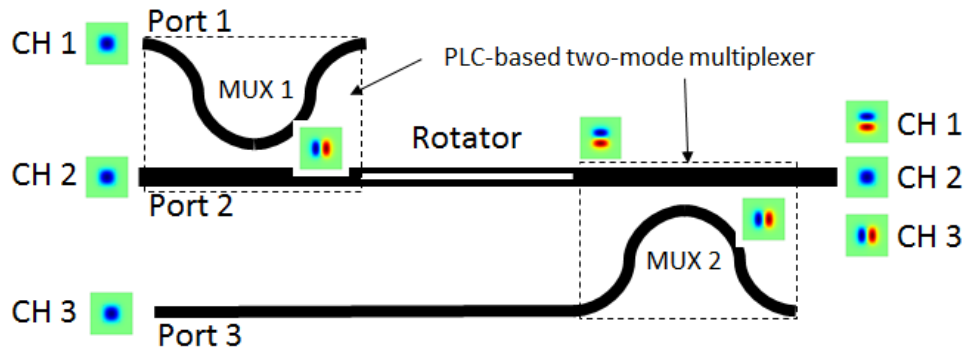| Index profile<br><br>Wavelength | With a trench | Without a trench |
|---|---|---|
| 1460 nm | | |
| 1480 nm | | |
| 1500 nm | | |
| 1520 nm | | |
| 1540 nm | | |
| 1550 nm | | |
| 1560 nm | | |
| 1580 nm | | |
| 1600 nm | | |

Fig. 12. Schematic drawing of PLC-based three-mode multiplexer that can multiplex and demultiplex $LP_{01}$, $LP_{11a}$, $LP_{11b}$ modes. The three-mode multiplexer consists of two PLC-based two-mode multiplexers and the proposed $LP_{11}$ mode rotator. Two-mode multiplexers are used for excitation of $LP_{11a}$ mode.

## 5. Conclusion

We have designed and fabricated the PLC-based $LP_{11}$ mode rotator for the excitation of $LP_{11b}$ mode. Numerical simulations showed that converting $LP_{11a}$ mode to $LP_{11b}$ mode could be achieved with high conversion efficiency (more than 90%) over a wide wavelength range from 1450 nm to 1650 nm. Numerical simulations also showed that the $LP_{11}$ mode rotator could convert $LP_{11b}$ mode to $LP_{11a}$ mode, had little polarization dependence, and had a good fabrication tolerance. It was clarified that the crosstalk to the undesired modes could be suppressed by making the trench smaller. We finally fabricated the proposed $LP_{11}$ mode rotator using silica-based PLC and confirmed that the fabricated $LP_{11}$ mode rotator can convert $LP_{11a}$ mode to $LP_{11b}$ mode over a wide wavelength range. We can realize the PLC-based three-mode (de)multiplexer for $LP_{01}$, $LP_{11a}$, and $LP_{11b}$ modes when we utilize the proposed $LP_{11}$ mode rotator and the two-mode (de)multiplexer [8].